RSC Advances

RSC Publishing

COMMUNICATION

Facile self-assembly of Au nanoparticles on a magnetic attapulgite/Fe_3O_4 composite for fast catalytic decoloration of dye

Cite this: *RSC Advances*, 2013, **3**, 11515

Received 17th April 2013,
Accepted 23rd May 2013

DOI: 10.1039/c3ra41836g

www.rsc.org/advances

Wenbo Wang,[ab] Fangfang Wang,[a] Yuru Kang[ab] and Aiqin Wang*[ab]

In this paper, we employed a simple and efficient electrostatic self-assembly strategy to fabricate superparamagnetic attapulgite/Fe_3O_4/Au nanoparticles (APT/Fe_3O_4/AuNPs) nanocomposites with a well-dispersed distribution of AuNPs using natural chitosan (CTS) as a ''bridge''. The ''toruloid'' APT/Fe_3O_4 composite with negative surface charges was firstly prepared by a one-step solvent-thermal reaction between APT, $FeCl_3$ and ethylene glycol, and then the positively charged CTS was used as a ''double sided tape'' to tightly adhere APT/Fe_3O_4 and AuNPs through electrostatic interaction. UV-vis, XRD and TEM analyses proved that the ''toruloid'' structure was formed, and AuNPs were successfully attached on the APT surface with good dispersion. The formation of the ''toruloid'' composite structure can not only bring stronger magnetism, but also facilitate the attachment of AuNPs. The APT/Fe_3O_4/AuNPs nanocomposite shows excellent catalytic activity, which can rapidly catalytically decolor a solution of Congo red (20 mg L^{-1}) within 2 min at a low dosage of 0.3 g L^{-1}. In addition, the nanocomposite shows strong magnetism with a maximum magnetization rate of 33.6 emu g^{-1}. This makes the nanocomposite prone to be magnetically separated and recycled.

1. Introduction

Gold nanoparticles (AuNPs) have received considerable attention in many frontier fields such as biomedicine,[1] sensing,[2] electronics,[3] smart materials,[4] surface-enhanced Raman scattering,[5] solar cell,[6] and catalysis,[7] *etc.* by virtue of their large surface area-to-volume ratio and higher interfacial activity. However, AuNPs are prone to aggregate due to the higher surface energy,[8] which greatly attenuates their activities and limits their extensive applications.

The immobilization of AuNPs on a nano-carrier provides an efficient approach to restrain aggregation, enhance stability, and reduce the cost.[9] The AuNPs may uniformly distribute and anchor on the carriers (*i.e.*, carbon nanotubes,[10] graphene,[11] nanofiber,[12] cellulose,[13] nanotubes,[14] nanospheres,[15] and nano-gel,[16] and Fe_3O_4,[17] *etc.*) with no risk of aggregation, and many hybrid materials have been developed. It was found that the structure, properties and stability of such materials can be flexibly adjusted by altering the type and surface character of the carriers.

Recently, natural nanoscale clay minerals, as a ''green material'', were considered as the preferred and promising carriers of AuNPs because they have plentiful surface groups and charges as well as abundant, low-cost, non-toxic and eco-friendly advantages.[18] The hybrid materials derived from nanoscale clays and AuNPs were especially concerned in the fields of catalysis due to the intrinsic higher stability and surface activity of clays.[19] The Si–O–Al or Si–O–Mg framework and Si–OH or Al–OH groups of clays may provide a Lewis active site, which facilitates to accelerate the transfer of electrons and enhance the catalytic activity of AuNPs. Hence, nano-clays were considered as an ideal and advantageous carrier of the catalyst. Of these, attapulgite (APT, called as palygorskite) is a special and representative natural one-dimensional nanoscale hydrated magnesium aluminum silicate clay mineral, with a 2 : 1 layer-ribbon composition, nanorod-like crystal structure, interpenetrated channel and plentiful Si–OH groups.[20] It was frequently used as a reinforce filler of nanocomposites,[21] adsorbents[22] and carriers.[23] As a carrier, the greater aspect ratio and surface charges of APT allow the assembly of various organic molecules, metal ions or nanoparticles onto its surface. The loading of Pd–CuO, Ag–AgBr, CeO_2/ZrO_2 nanoparticles on APT generate hybrid materials with satisfactory catalytic activities, low-cost and eco-friendly advantages.[24] The combination of APT with magnetic Fe_3O_4 nanoparticles also produce composite that is prone to be separated from solution.[25] It is expected that the combination of APT, Fe_3O_4 and AuNPs can build new nanocomposite with excellent catalytic properties, stable structure, recyclable and eco-friendly advantages. However, there are rare researches on the design and development of such nanocomposite materials.

For this purpose, we employed a simple and efficient electrostatic self-assembly strategy to anchor AuNPs onto the magnetic APT/Fe_3O_4 composite, using chitosan (CTS) as the green

[a]*Center of Eco-material and Green Chemistry, Lanzhou Institute of Chemical Physics, Chinese Academy of Science, Lanzhou, 730000, P. R. China*
[b]*R&D Center of Xuyi Attapulgite Applied Technology, Lanzhou Institute of Chemical Physics, Chinese Academy of Science, Lanzhou 730000, P. R. China.*
E-mail: aqwang@licp.cas.cn; Fax: +86-931-8277088; Tel: +86-931-4968118

"bridge". The "toruloid" APT/Fe_3O_4 nanocomposite with negative charges was firstly prepared through a one-step solvent-thermal reaction, and then the positively charged CTS was used as a medium to adhere APT/Fe_3O_4 and AuNPs by strong electrostatic interaction. The structure, morphologies and magnetism of the nanocomposite were characterized by UV-vis spectroscopy (UV-vis), X-ray diffraction (XRD), transmission electron microscopy (TEM), and vibrating sample magnetometry, and the catalytic activity was systematically evaluated using the catalytic reducing action of CR as the model system.

2. Experimental

Materials

APT with the composition CaO 1.29%, Al_2O_3 9.69%, Na_2O 0.48%, MgO 10.94%, SiO_2 51.75%, 0.99% K_2O and 5.04% Fe_2O_3, determined by a Minipal4 X-Ray fluorescence spectrometer (PANalytical Co., Netherland), was produced by Mingguang minerals located on Anhui, China. Chitosan (CTS) with a degree of deacetylation (DD) of 90% and molecular weight of 600 kDa was from Yuhuan Ocean Biology Company (Zhejiang, China). $FeCl_3{\cdot}6H_2O$, ethylene glycol, sodium acetate, acetic acid, poly (ethylene glycol), chloroauric acid ($HAuCl_4$) and sodium borohydride ($NaBH_4$) were purchased from Sinopharm Chemical Reagent Co., Ltd. (Shanghai, China), and used without further purification. Congo red (CR) was purchased from Alfa Aesar and used as received. All other reagents used were of analytical grade and all solutions were prepared with ultrapure water (18.25 MΩ cm).

Preparation of APT/Fe_3O_4 composite

The APT/Fe_3O_4 composite was prepared by a modified procedure described previously.[26] Generally, $FeCl_3{\cdot}6H_2O$ (2.0 g) was dissolved in 60 mL ethylene glycol to form a clear solution, and then the precipitator sodium acetate (5.0 g) and the surfactant poly(ethylene glycol) (1.2 g) were added. After the mixture solution was stirred for 60 min, 0.6 g APT was added and the mixture was further stirred for 3 h to form a homogeneous suspension. Finally, the mixture was transferred into a 100 mL Teflon-lined stainless steel autoclave, and reaction at 180 °C for 12 h. After cooling the autoclave to room temperature, the obtained black product (APT/Fe_3O_4) was magnetically separated, and successively washed with methanol and ultrapure water 5 times, respectively, and the product was dried at 40 °C under vacuum.

Self-assembly of AuNPs onto APT/Fe_3O_4

AuNPs were prepared by reducing $HAuCl_4$ using $NaBH_4$ in the presence of sodium citrate. Typically, 10 mL of the $HAuCl_4$ solution (1%, *m*/*v*) was added to 900 mL ultrapure water in a beaker. Then, 20 mL of the aqueous solution of sodium citrate (1 wt%) was added. After stirred for 5 min, 10 mL of the freshly prepared $NaBH_4$ solution (0.075 wt%) was rapidly added, and the purple–red solution was obtained and cured for 2 h. The concentration of AuNPs sols is 0.3129 mmol L^{-1}.

The self-assembly of AuNPs on APT/Fe_3O_4 can be easily achieved using CTS as the "bridge". Typically, 1 g of the negatively charged APT/Fe_3O_4 was soaked in 500 mL 0.1 wt% CTS solution, and then stirred at room temperature for 24 h to reach the saturation adsorption of APT/Fe_3O_4 for CTS. The resultant CTS-modified Fe_3O_4/APT was separated by a magnet and successively washed with 1% aqueous solution of acetic acid and ultra-pure water 3 times. Then, the purple–red solution of AuNPs was gradually added to the beaker containing CTS-modified APT/Fe_3O_4. Due to the rapid adsorption of CTS-modified APT/Fe_3O_4 for AuNPs, the added solution will immediately become colorless. The addition process was continued until the solution does not fade again with adding the solution of AuNPs (adsorption saturation was reached). The resultant black–purple APT/Fe_3O_4/AuNPs product was magnetically separated and washed with ultrapure water, and then dried at 50 °C under vacuum.

Evaluation of catalytic activity

Catalytic reduction reaction of CR was used to evaluate the catalytic activity of the nanocomposite. Typically, 0.03 g APT/Fe_3O_4/AuNPs nanocomposite was added into 100 mL CR solution (20 mg L^{-1}) with and without 15 mmol L^{-1} $NaBH_4$. After set time intervals, the nanocomposites were instantly separated from the solution by suction filtering through a filter (0.45 μm). The UV-vis spectra of the solution were scanned at 25 °C in the range 300–800 nm and the absorbance was determined at 504 nm using a quartz cell (1 cm path length). The absorbance was defined as a criterion to evaluate the decoloration efficiency.

The solid was collected, washed with distilled water 3 times and dried under vacuum, and then used for another catalytic cycle. The same procedure was repeated 10 times to evaluate the reusability of the nanocomposites.

Calculation of reduction rate constants

The catalytic reduction rate of dyes catalyzed by APT/Fe_3O_4/AuNPs nanocomposites was calculated using the following equation.

$$\mathrm{Ln}(C/C_0) = -K_{\mathrm{obs}}t \quad (1)$$

where C (mg L^{-1}) is the concentration of dye at time t, C_0 (mg L^{-1}) is the initial concentration of dye, and K_{obs} is the first order rate constant.[27]

Characterization

UV-vis spectra were determined using a UV-visible spectrophotometer (SPECORD 200, Analytik Jera AG). XRD patterns were collected on a Philip X'Pert Pro diffractometer using Cu-Kα radiation of 1.5406 Å (40 kV, 30 mA). The morphologies of the samples were observed using a JEM-1200 EX/S transmission electron microscope (TEM) (JEOL, Tokyo, Japan), and the sample was ultrasonically dispersed in absolute ethanol and dropped onto a micro grid before observation. Zeta potentials were determined on a Malvern Zetasizer Nano system with irradiation from a 633 nm He–Ne laser (ZEN3600).

3. Results and discussion

APT/Fe_3O_4/AuNPs nanocomposites

The AuNPs were successfully prepared using sodium citrate as a stabilizer, and their formation was proved by surface plasmon resonance peak at 520 nm (UV-vis spectra) (Fig. 1).[28] The AuNPs

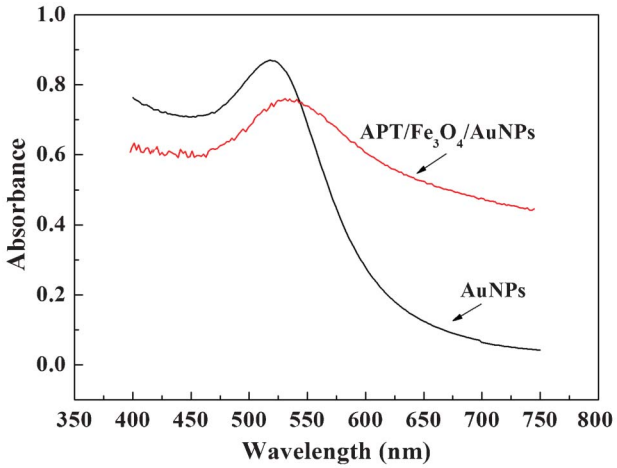

Fig. 1 The UV-vis spectra of AuNPs and APT/Fe_3O_4/AuNPs.

with negative charges (functionalized by $-COO^-$ groups) can self-assemble onto CTS-modified APT/Fe_3O_4 to form a nanocomposite, and the electrostatic interaction is the main driving force (Scheme 1). The Zeta potentials of APT/Fe_3O_4 and AuNPs are −22.8 and −23.4 mV, respectively. After modifying APT/Fe_3O_4 with CTS, the positively charged CTS polymer chains may attach on the surface of APT/Fe_3O_4, and the CTS-modified APT/Fe_3O_4 becomes electropositive with a Zeta potential of +55.6 mV. The positively charged surface may strongly adsorb negatively charged AuNPs to form a stable combination, and the appearance of an absorbance peak at 530 nm on the UV-vis spectra of APT/Fe_3O_4/AuNPs also proved the attachment of AuNPs (Fig. 1).

Fig. 2 shows the XRD curves of APT, APT/Fe_3O_4 and APT/Fe_3O_4/AuNPs, which provided a direct evidence for the attachment of AuNPs on the APT/Fe_3O_4 composite. As can be seen, APT shows a characteristic diffraction at $2\theta = 8.41^\circ$ (d = 1.0493 nm, 1 1 0), $2\theta = 13.75^\circ$ (d = 0.6443 nm, 2 0 0), $2\theta = 16.42^\circ$ (d = 0.5401 nm, 1 3 0), $2\theta = 19.89^\circ$ (d = 0.4466 nm, 0 4 0) and $2\theta = 21.48^\circ$ (d = 0.4138 nm, 3 1 0).[29] After solvent-thermal reaction, the new diffraction peaks at $2\theta = 18.28$ (d = 0.4855 nm, 1 1 1), at $2\theta = 30.18^\circ$ (d = 0.2962 nm, 2 2 0), 35.57° (d = 0.2525 nm, 2 0 0), 43.13° (d = 0.2098 nm, 4 0 0), 53.408° (d = 0.1714 nm, 4 2 2) and 57.04° (d = 0.1615 nm, 5 1 1) were observed in the XRD curves of the product, which could be ascribed to the characteristic diffraction peaks of the face-centered cubic phase of Fe_3O_4,[30] with the space group *Fd3m* and lattice parameters $a = b = c$ = 0.8391 nm (JCPDF No. 88-0315). This indicates that the APT/Fe_3O_4 composite was formed during the solvent-thermal reaction. The characteristic diffraction peaks of AuNPs at $2\theta = 38.26^\circ$ (1 1 1) and 45.05° (2 0 0)[31] (JCPDF No. 04-0784), also appeared in the XRD curves of the nanocomposite. This indicates that the AuNPs were attached on the surface of the APT/Fe_3O_4 composite, which is consistent with the UV-vis results. Whereas the position of 1 1 0 characteristic diffraction peaks of APT (the basal plane of the APT structure) has no obvious change, indicating the crystal structure of APT has not been destroyed during the synthesis process.

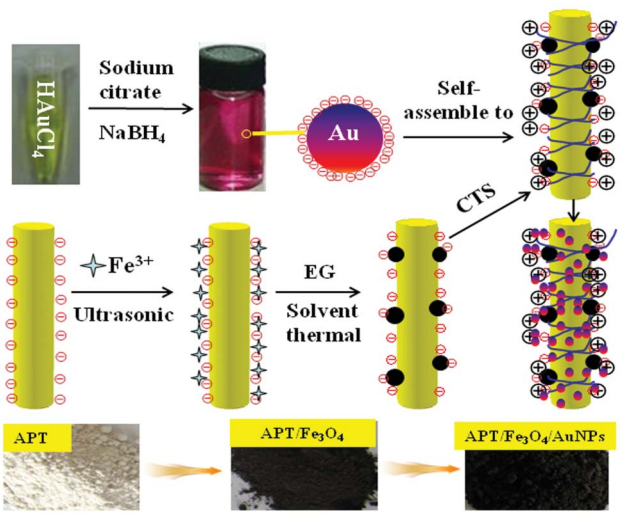

Scheme 1 The proposed formation mechanism of APT/Fe_3O_4/AuNPs.

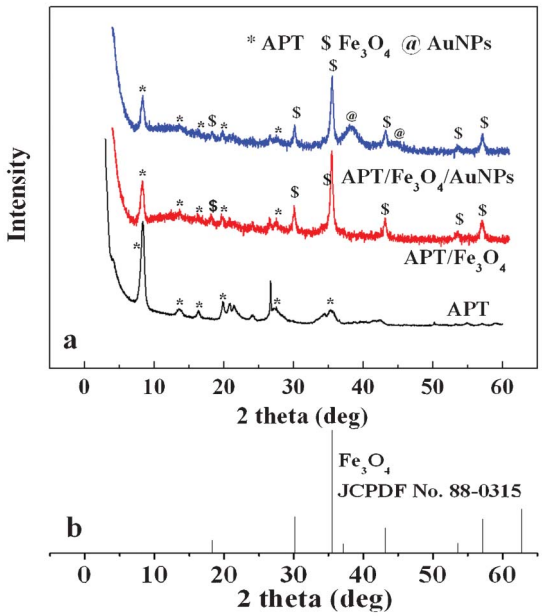

Fig. 2 (a) XRD patterns of APT, APT/Fe_3O_4 and APT/Fe_3O_4/AuNPs; and (b) the standard XRD pattern of Fe_3O_4.

Fig. 3 shows the TEM images of APT/Fe_3O_4 and APT/Fe_3O_4/AuNPs. It can be clearly observed that the black spherical Fe_3O_4 was anchored on the external surface of APT to form a "toruloid" compound structure (Fig. 3a). The advantage of such a structure is: the Fe_3O_4 spheres only occupy a small fraction of the APT surface, and so the surface properties of APT can be retained to a greater degree. Some organic matters can be observed on the surface of both APT and Fe_3O_4, indicating that the APT/Fe_3O_4 composite was successfully modified with CTS (Fig. 3b). After contact with negatively charged AuNPs, the $-NH_3^+$ groups of CTS-modified APT/Fe_3O_4 composite may attract AuNPs by electrostatic interaction and form a stable compound structure, which can be confirmed by the appearance of nanoparticles on the surface of CTS-modified APT/Fe_3O_4 composite (Fig. 3b). This result reveals that the AuNPs can be successfully anchored on the APT/Fe_3O_4 composite using

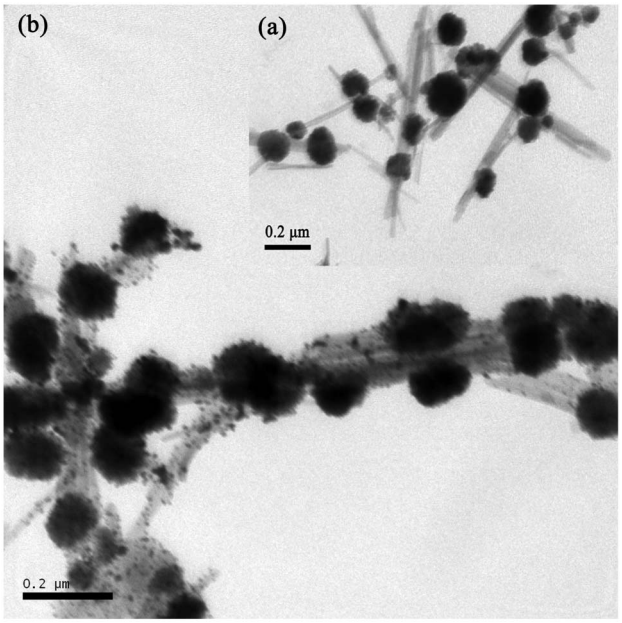

Fig. 3 TEM images of (a) APT/Fe_3O_4 and (b) APT/Fe_3O_4/AuNPs.

CTS as a medium, and the nanocomposite was fabricated by a simple and mild approach.

The magnetic hysteresis loop for APT/Fe_3O_4/AuNPs is shown in Fig. 4. Neither remanence nor coercivity is observed, indicating the superparamagnetic property of the nanocomposite.[32] The saturation magnetization of the nanocomposite is 33.6 emu g^{-1}, which is enough to guarantee the thorough separation of the nanocomposite from the solution by a magnet after the catalytic reaction (the inset in Fig. 4).

Catalytic properties

The incorporation of AuNPs endows the APT/Fe_3O_4 composite with excellent catalytic properties. In this section, the catalytic activity of the APT/Fe_3O_4/AuNPs nanocomposite was evaluated using the catalytic reduction of an anionic dye CR as a model reaction. As shown in Fig. 5(a), the addition of $NaBH_4$ to CR solutions does not affect the absorbance of CR solution. This indicates that BH_4^- ions cannot reduce the CR dye in the absence of the nanocomposite. After only adding the nanocomposite

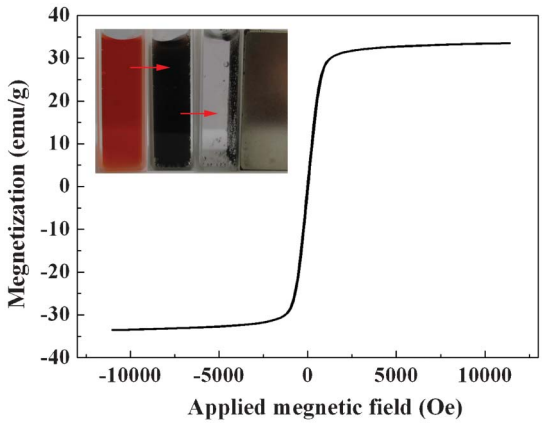

Fig. 4 The magnetic hysteresis loops of APT/Fe_3O_4/AuNPs. The inset indicates the catalytic decoloration effect and the efficient magnetic separation.

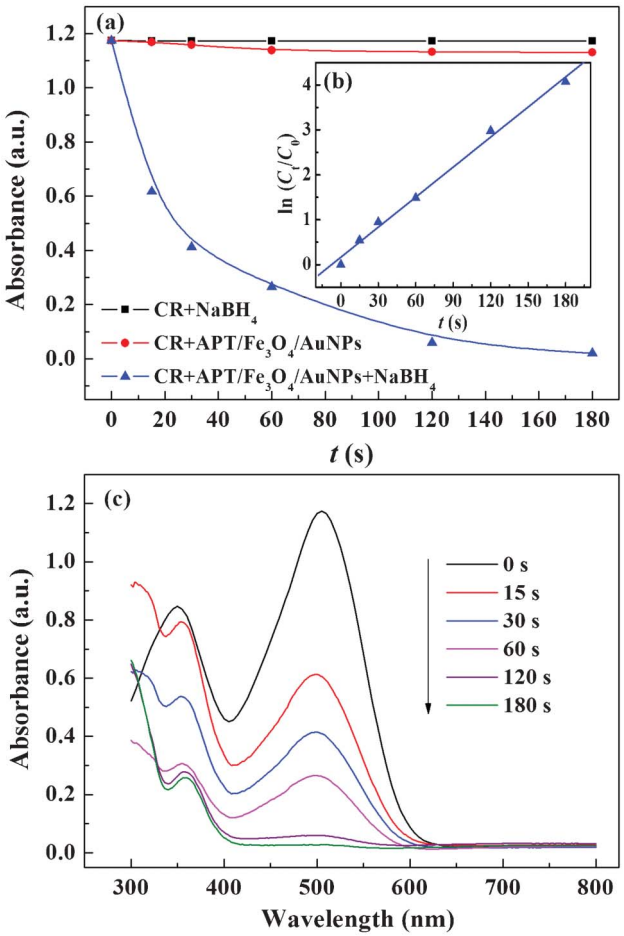

Fig. 5 (a) The plots of absorbance against time for CR dye reductions catalyzed by APT/Fe_3O_4/AuNPs (initial CR concentration, 20 mg L^{-1}; initial $NaBH_4$ concentration, 15 mM; initial dosage, 0.3 g L^{-1}); and (b) the dependent UV-vis spectra for the reduction of CR by $NaBH_4$ in the presence of APT/Fe_3O_4/AuNPs.

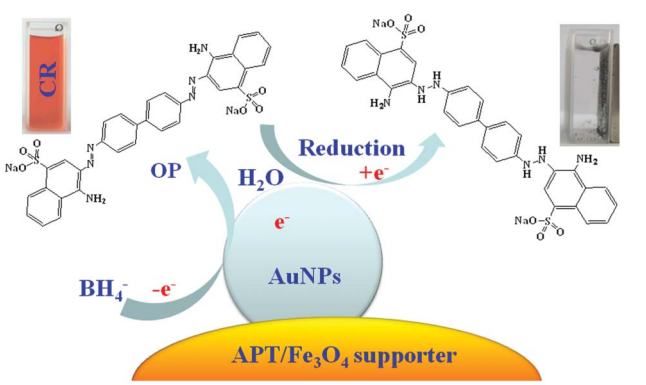

Scheme 2 Proposed mechanisms for the catalytic reduction of CR dye by $NaBH_4$ using APT/Fe_3O_4/AuNPs as the catalyst (OP represents the oxidative product).

Table 1 Comparison of decoloration efficiency for CR dye using various decoloration protocols

Decoloration protocol	Materials	Dosage (g L^{-1})	Initial conc. (mg L^{-1})	Decoloration time	Ref.
Photocatalytic	Chitosan/nano-CdS	1.5	20	180 min	33*a*
Photocatalytic	TiO_2	1.0	55	480 min	33*b*
Anaerobic & catalysis	Anaerobic aludge + AQDS	1.5	209	33 d	33*c*
Enzyme	Laccase/CS/glass beads	0.1	200	192 h	33*d*
Photochemical	UV/H_2O_2	1.7	50	60 min	33*e*
Adsorption	$KxMnO_2/TiO_2$	1.0	10	120 min	33*f*
Adsorption	Ca-bentonite	2.0	100	180 min	33*g*
Catalytic reduction	APT/Fe_3O_4/AuNPs	0.3	20	2 min	This work

(without $NaBH_4$), the absorbance was slightly decreased due to the weak adsorption of the nanocomposite for CR dye. No obvious decoloration was observed. This indicates that the catalyst and the reductant are essential to the reducing decoloration of the CR dye. However, when the APT/Fe_3O_4/AuNPs nanocomposite was added to the CR solution containing BH_4^- ions, the absorbance of the solution at 504 nm was rapidly decreased to the value close to zero within 2 min (Fig. 5c), and the red color of the solution was rapidly faded (as is also intuitively shown by the digital photos shown in Fig. 4 and Scheme 2). The experimental data was fitted by eqn (1) for calculating the rate constant K_{obs}. The plots of $-\ln(C_t/C_0)$ *vs* t give better straight lines. The K_{obs} value can be calculated by the slop of straight line (Fig. 5b), and the K_{obs} value is 0.1662 s^{-1} (R = 0.9989) for the nanocomposite. Table 1 listed the conventionally used approaches for the decoloration of CR dye and their decoloration efficiency. By contrast, the catalytic reduction using APT/Fe_3O_4/AuNPs as the catalyst can decolor CR solution within shorter time, which reflects the relatively higher decoloration efficiency. These results indicate that the nanocomposite can be used a highly-efficient catalyst for the reducing decoloration of the CR dye.

It can also be noticed from Fig. 5c that the absorbance of the CR at 350 nm was shifted to 359 nm along with the disappearance of the absorbance peak at 540 nm, which implies that the azo CR molecules were reduced to form a new product. Scheme 2 shows the proposed catalytic reduction mechanism. It was shown that the AuNPs trigger the reducing decoloration of CR solution by relaying electron from the BH_4^- donor to AuNPs, and then conveying electrons to the acceptor CR molecules.[34] As a result, the azo double –N=N– bonds were reduced as the –N–N– bonds, and the color of CR was faded.[34]

As a catalysis material, the reusability of the nanocomposite is especially important for its practical application. Fig. 6 shows the reducing percentage of dye after catalytic reduction at the time 2 min, repeated for 10 cycles. It can be observed that the reducing ratio has no obvious decrease, and the reduction percentage still reached 98% of the initial values. This indicates that the nanocomposite has satisfactory cycling stability and can be used as potential catalysis materials for various applications.

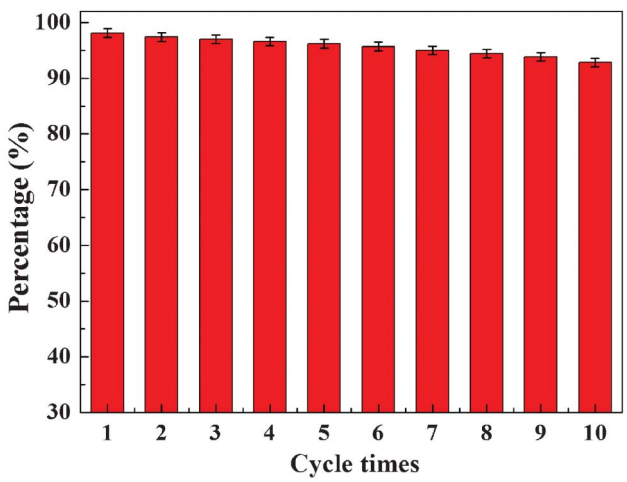

Fig. 6 The catalytic properties of the nanocomposite after repeating 10 times.

4. Conclusion

Superparamagnetic APT/Fe_3O_4/AuNPs nanocomposites with a well-dispersed distribution of AuNPs on the surfaces of the APT/Fe_3O_4 composite were fabricated by a facile self-assembly approach using CTS as the green "bridge". UV-vis, XRD and TEM analysis proved that the APT/Fe_3O_4 composite with "toruloid" morphology was formed by one-step solvent-thermal reaction, and the AuNPs were tightly anchored on the surface of APT/Fe_3O_4 without aggregation. The "toruloid" structure composed of APT "string" and Fe_3O_4 "beads" can not only bring strong magnetism, but also restrain the surface activity of APT to a greater degree. CTS was uniformly attached on the surface of APT/Fe_3O_4, which facilitates the assembly of AuNPs with uniform distribution. The nanocomposites can be used as a highly active and recyclable catalyst for the catalytic reducing decoloration of CR dye, and the CR solution (20 mg L^{-1}) was rapidly decolored within 2 min at a low dosage of 0.3 g L^{-1}. The catalytic activity has no obvious decrease after being used for 10 cycles. As a whole, the reported method is quite simple, and the strategy can be extended for the fabrication of various nanoparticles/clays matrix nanocomposites with different structures, properties and eco-friendly advantages, and their application fields can be extended to separation, hydrogen storage, drug delivery, electrode materials for fuel cells, and so on.

Acknowledgements

We would like to thank the "863" Project of the Ministry of Science and Technology, China (No. 2013AA031403), Technology Support Project of Jiangsu Provincial Sci. & Tech.

Department (No. BE2012113) and the Open Fund of the Xuyi Center of Attapulgite Applied Technology Research Development & Industrialization, Chinese Academy of Sciences (No. CASXY-04).

References

1 (*a*) E. C. Dreaden, A. M. Alkilany, X. H. Huang, C. J. Murphy and M. A. El-Sayed, *Chem. Soc. Rev.*, 2012, **41**, 2740–2779; (*b*) P. Joshi, S. Chakraborti, J. E. Ramirez-Vick, Z. A. Ansari, V. Shanker, P. Chakrabarti and S. P. Singh, *Colloids Surf., B*, 2012, **95**, 195–200.

2 (*a*) K. Saha, S. S. Agasti, C. Kim, X. N. Li and V. M. Rotello, *Chem. Rev.*, 2012, **112**, 2739–2779; (*b*) X.-W. Liu, F.-Y. Wang, F. Zhen and J.-R. Huang, *RSC Adv.*, 2012, **2**, 7647–7651.

3 (*a*) C. Gutiérrez-Sánchez, M. Pita, C. Vaz-Domínguez, S. Shleev and A. L. De Lacey, *J. Am. Chem. Soc.*, 2012, **134**, 17212–17220; (*b*) Y. X. Li, J. T. Cox and B. Zhang, *J. Am. Chem. Soc.*, 2010, **132**, 3047–3054.

4 (*a*) C. O. Baker, B. Shedd, R. J. Tseng, A. A. Martinez-Morales, C. S. Ozkan, M. Ozkan, Y. Yang and R. B. Kaner, *ACS Nano*, 2011, **5**, 3469–3474; (*b*) M. S. Strozyk, M. Chanana, I. Pastoriza-Santos, J. Pérez-Juste and L. M. Liz-Marzán, *Adv. Funct. Mater.*, 2012, **22**, 1322.

5 C.-C. Chang, K.-H. Yang, Y.-C. Liu and T.-C. Hsu, *Colloids Surf., B*, 2012, **93**, 169–173.

6 D. H. Wang, D. Y. Kim, K. W. Choi, J. H. Seo, S. Hyuk Im, J. H. Park, O. O. Park and A. J. Heeger, *Angew. Chem.*, 2011, **123**, 5633–5637.

7 (*a*) M. Stratakis and H. Garcia, *Chem. Rev.*, 2012, **112**, 4469–4506; (*b*) R. Fenger, E. Fertitta, H. Kirmse, A. F. Thünemann and K. Rademann, *Phys. Chem. Chem. Phys.*, 2012, **14**, 9343–9349.

8 C. Zhu, L. Han, P. Hu and S. Dong, *Nanoscale*, 2012, **4**, 1641–1646.

9 (*a*) M. Lee, S. C. Hong and D. Kim, *Carbon*, 2012, **50**, 2465–2471; (*b*) M. D. L. Ruiz Peralta, U. Pal and R. S. Zeferino, *ACS Appl. Mater. Interfaces*, 2012, **4**, 4807–4816.

10 (*a*) F. B. Lollmahomed and R. Narain, *Langmuir*, 2011, **27**, 12642–12649; (*b*) Z. Zanolli, R. Leghri, A. Felten, J.-J. Pireaux, E. Llobet and J.-C. Charlier, *ACS Nano*, 2011, **5**, 4592–4599.

11 (*a*) W. J. Hong, H. Bai, Y. X. Xu, Z. Y. Yao, Z. Z. Gu and G. G. Shi, *J. Phys. Chem. C*, 2010, **114**, 1822–1826; (*b*) X. G. Xie, J. J. Long, J. Xu, L. M. Chen, Y. Wang, Z. Z. Zhang and X. X. Wang, *RSC Adv.*, 2012, **2**, 12438–12446.

12 H. G. Kang, Y. H. Zhu, X. L. Yang, J. H. Shen, C. Chen and C. Z. Li, *New J. Chem.*, 2010, **34**, 2166–2175.

13 E. Lam, S. Hrapovic, E. Majid, J. H. Chong and J. H. T. Luong, *Nanoscale*, 2012, **4**, 997–1002.

14 (*a*) F.-X. Xiao, *RSC Adv.*, 2012, **2**, 12699–12701; (*b*) Z. Y. Zhang, C. L. Shao, P. Zou, P. Zhang, M. Y. Zhang, J. B. Mu, Z. C. Guo, X. H. Li, C. H. Wang and Y. C. Liu, *Chem. Commun.*, 2011, **47**, 3906–3908.

15 S. T. Kochuveedu, D.-P. Kim and D. H. Kim, *J. Phys. Chem. C*, 2012, **116**, 2500–2506.

16 E. Marsich, A. Travan, I. Donati, A. D. Luca, M. Benincasa, M. Crosera and S. Paoletti, *Colloids Surf., B*, 2011, **83**, 331–339.

17 E. D. Smolensky, M. C. Neary, Y. Zhou, T. S. Berquo and V. C. Pierre, *Chem. Commun.*, 2011, **47**, 2149–2151.

18 (*a*) V. Belova, D. V. Andreeva, H. Möhwald and D. G. Shchukin, *J. Phys. Chem. C*, 2009, **113**, 5381–5389; (*b*) D. Varade and K. Haraguchi, *J. Mater. Chem.*, 2012, **22**, 17649–17655.

19 (*a*) S. Letaief, W. Pell and C. Detellier, *Can. J. Chem.*, 2011, **89**, 845–853; (*b*) A. Álvarez, S. Moreno, R. Molina, S. Ivanova, M. A. Centeno and J. A. Odriozola, *Appl. Clay Sci.*, 2012, **69**, 22–29.

20 V. A. Drits and G. V. Sokolova, *Sov. Phys. Crystallogr.*, 1971, **16**, 183–185.

21 D. J. Huang, W. B. Wang, J. X. Xu and A. Q. Wang, *Chem. Eng. J.*, 2012, **210**, 166–172.

22 J. Zhang, S. D. Xie and Y.-S. Ho, *J. Hazard. Mater.*, 2009, **165**, 218–222.

23 X. He, A. D. Tang, H. M. Yang and J. Ouyang, *Appl. Clay Sci.*, 2011, **53**, 80–84.

24 (*a*) C. L. Huo and H. M. Yang, *Appl. Clay Sci.*, 2013, **74**, 87–94; (*b*) Y. Q. Yang and G. K. Zhang, *Appl. Clay Sci.*, 2012, **67–68**, 11–17.

25 (*a*) J. M. Pan, L. C. Xu, J. D. Dai, X. X. Li, H. Hang, P. W. Huo, C. X. Li and Y. S. Yan, *Chem. Eng. J.*, 2011, **174**, 68–75; (*b*) Y. S. Liu, P. Liu, Z. X. Su, F. S. Li and F. S. Wen, *Appl. Surf. Sci.*, 2008, **255**, 2020–2025.

26 A. D. Bokare, R. C. Chikate, C. V. Rode and K. M. Paknikar, *Appl. Catal., B*, 2008, **79**, 270–278.

27 G. H. Zhao, J. Z. Wang, Y. F. Li, X. Chen and Y. P. Liu, *J. Phys. Chem. C*, 2011, **115**, 6350–6359.

28 W. Haiss, N. T. K. Thanh, J. Aveyard and D. G. Fernig, *Anal. Chem.*, 2007, **79**, 4215–4221.

29 W. C. Yan, D. Liu, D. Y. Tan, P. Yuan and M. Chen, *Spectrochim. Acta, Part A*, 2012, **97**, 1052–1057.

30 (*a*) G. M. Zhou, D. W. Wang, F. Li, L. L. Zhang, N. Li, Z. S. Wu, L. Wen, G. Q. Lu and H. M. Cheng, *Chem. Mater.*, 2010, **22**, 5306–5313; (*b*) S. X. Zhang, X. L. Zhao, H. Y. Niu, Y. L. Shi, Y. Q. Cai and G. B. Jiang, *J. Hazard. Mater.*, 2009, **167**, 560–566.

31 X. H. Liu, J. Zhang, X. Z. Guo, S. R. Wang and S. H. Wu, *RSC Adv.*, 2012, **2**, 1650–1655.

32 J. Y. Park, P. Daksha, G. H. Lee, S. Woo and Y. M. Chang, *Nanotechnology*, 2008, **19**, 365603–365609.

33 (*a*) H. Y. Zhu, R. Jiang, L. Xiao, Y. H. Chang, Y. J. Guan, X. D. Li and G. M. Zeng, *J. Hazard. Mater.*, 2009, **169**, 933–940; (*b*) L. Ćurković, D. Ljubas and H. Juretić, *Reac. Kinet. Mech. Cat.*, 2012, **99**, 201–208; (*c*) M. C. Costa, S. Mota, R. F. Nascimento and A. B. Dos Santos, *Bioresour. Technol.*, 2010, **101**, 105–110; (*d*) A. Sadighi and M. A. Faramarzi, *J. Taiwan Inst. Chem. Eng.*, 2013, **44**, 156–162; (*e*) D. Kamel, A. Sihem, C. Halima and S. Tahar, *Desalination*, 2009, **247**, 412–422; (*f*) Y. Q. Dai, X. F. Lu, M. McKiernan, E. P. Lee, Y. M. Sun and Y. N. Xia, *J. Mater. Chem.*, 2010, **20**, 3157–3162; (*g*) L. L. Lian, L. P. Guo and C. J. Guo, *J. Hazard. Mater.*, 2009, **161**, 126–131.

34 W. Li, J. Li, W. B. Qiang, J. J. Xu and D. K. Xu, *Analyst*, 2013, **138**, 760.

